Toxicology 257 (2009) 161–171

Contents lists available at ScienceDirect

Toxicology

journal homepage: www.elsevier.com/locate/toxicol

Oxidative stress and inflammatory response in dermal toxicity of single-walled carbon nanotubes

A.R. Murray[a,b,*], E. Kisin[a], S.S. Leonard[a], S.H. Young[a], C. Kommineni[a], V.E. Kagan[c], V. Castranova[a,b], A.A. Shvedova[a,b,*]

[a] PPRB/NIOSH, Morgantown, WV, United States
[b] Department of Physiology and Pharmacology, WVU, United States
[c] Center for Free Radical and Antioxidant Health, Department of Environmental and Occupational Health, University of Pittsburgh, Pittsburgh, PA, United States

ARTICLE INFO

Article history:
Received 13 October 2008
Received in revised form 16 December 2008
Accepted 18 December 2008
Available online 30 December 2008

Keywords:
Single-walled nanotubes
Oxidative stress
Glutathione
Skin
Electron spin resonance

ABSTRACT

Single-walled carbon nanotubes (SWCNT) represent a novel material with unique electronic and mechanical properties. The extremely small size (~1 nm diameter) renders their chemical and physical properties unique. A variety of different techniques are available for the production of SWCNT; however, the most common is via the disproportionation of gaseous carbon molecules supported on catalytic iron particles (high-pressure CO conversion, HiPCO). The physical nature of SWCNT may lead to dermal penetration following deposition on exposed skin. This dermal deposition provides a route of exposure which is important to consider when evaluating SWCNT toxicity. The dermal effects of SWCNT are largely unknown. We hypothesize that SWCNT may be toxic to the skin. We further hypothesize that SWCNT toxicity may be dependent upon the metal (particularly iron) content of SWCNT via the metal's ability to interact with the skin, initiate oxidative stress, and induce redox-sensitive transcription factors thereby affecting/leading to inflammation. To test this hypothesis, the effects of SWCNT were assessed both *in vitro* and *in vivo* using EpiDerm FT engineered skin, murine epidermal cells (JB6 P+), and immune-competent hairless SKH-1 mice. Engineered skin exposed to SWCNT showed increased epidermal thickness and accumulation and activation of dermal fibroblasts which resulted in increased collagen as well as release of pro-inflammatory cytokines. Exposure of JB6 P+ cells to unpurified SWCNT (30% iron) resulted in the production of ESR detectable hydroxyl radicals and caused a significant dose-dependent activation of AP-1. No significant changes in AP-1 activation were detected when partially purified SWCNT (0.23% iron) were introduced to the cells. However, NFκB was activated in a dose-dependent fashion by exposure to both unpurified and partially purified SWCNT. Topical exposure of SKH-1 mice (5 days, with daily doses of 40 μg/mouse, 80 μg/mouse, or 160 μg/mouse) to unpurified SWCNT caused oxidative stress, depletion of glutathione, oxidation of protein thiols and carbonyls, elevated myeloperoxidase activity, an increase of dermal cell numbers, and skin thickening resulting from the accumulation of polymorphonuclear leukocytes (PMNs) and mast cells. Altogether, these data indicated that topical exposure to unpurified SWCNT, induced free radical generation, oxidative stress, and inflammation, thus causing dermal toxicity.

Published by Elsevier Ireland Ltd.

1. Introduction

Nanotechnology is a rapidly emerging field resulting in the discovery of unique materials with a variety of applications from electronics to engineered tissues (Roco et al., 2000). A variety of nanoparticles exist; however, single-walled carbon nanotubes (SWCNT) have elicited a large interest due to their unique mechanical and chemical properties. Along with extraordinary electronic, light-emitting, and catalytic properties, SWCNT have potential applications in high-strength materials, reinforced rods, quantum wires, mechanical memory, and microfabrication of conjugated polymers (Subramoney, 1998; Sinnott and Andrews, 2001).

Individual nanotubes, which are formed as a single wall of carbon atoms, have a diameter as small as 1.5 nm and lengths of 1–100 μm. The manufacturing of SWCNT relies on the use of transition-metal catalysts resulting in the presence of up to 30% metal catalyst by mass in raw SWCNT (Maynard et al., 2004). The catalysts predominately used are iron (Fe), nickel (Ni), and cobalt (Co). Further processing is capable of removing most of the catalytic component; however, some of the metal catalyst is completely or partially encased within the carbon nanotubes making complete removal of the metal impossible without destroying the nanotubes

* Corresponding authors at: Health Effects Laboratory Division, Pathology and Physiology Research Branch, NIOSH, M/L 2015, 1095 Willowdale Road, Morgantown, WV 26505, United States. Tel.: +1 304 285 6177; fax: +1 304 285 5938.
E-mail addresses: zsk1@cdc.gov (A.R. Murray), ats1@cdc.gov (A.A. Shvedova).

0300-483X/$ – see front matter. Published by Elsevier Ireland Ltd.
doi:10.1016/j.tox.2008.12.023

(Maynard et al., 2004). As a result, the health risks associated with nanotube materials may be due to both the carbonaceous and metallic components. The transition-metal complexes as well as free Fe, Ni, and Co are known to be catalysts of biological free radical reactions. The unique properties and size of carbon nanoparticles may also result in unique health risks (Borm, 2002), which are not able to be predicted by the toxicological effects of larger particulates of the same composition. Therefore, introduction of novel materials into industry requires safety evaluation as well as an understanding of the impact of the nanomaterials on human health.

Dermal deposition has the potential to be a major route of exposure during the manufacturing, use, and disposal of SWCNT. It has been shown that exposure to carbon black, carbon black fibers, and man-made fibers in humans causes dermal irritation, hyperkeratosis, pruritus, and dermatitis (Capusan and Mauksch, 1969; Komarova, 1965; Eedy, 1996; Thriene et al., 1996). However, limited literature exists evaluating the toxic effects of SWCNT to the skin. Previous work by our lab has shown that unpurified SWCNT induces cytotoxicity in human keratinocytes (Shvedova et al., 2003). Our central hypothesis is that SWCNT may be toxic to the skin with the toxicity dependent upon the formation of free radicals, and induction of oxidative stress due to catalytic metals present in raw SWCNT. Because inflammation provides a redox environment in which transition metals, e.g. iron, can fully realize their pro-oxidant capacity via Fenton reaction, a combination of an inflammatory response with catalytically competent transition metals will synergistically enhance damage to cells and tissue. To address these questions, we studied the effects of SWCNT in engineered skin, murine epidermal JB6 P+ cells and skin of SKH-1 mice. We used ESR spectroscopy to detect ROS production upon addition of SWCNT to JB6 P+ cells. Additionally, we tested the effects of SWCNT using bio-engineered skin tissue assessing release of pro-inflammatory cytokines along with changes in engineered skin structure. SWCNT toxicity was assessed by the measurement of oxidative stress in JB6+ cells and the skin of SKH-1 mice topically exposed to SWCNT by evaluating decreases in antioxidants, increases in lipid and protein oxidative products, as well as changes in skin morphology assessed by inflammatory and mast cell influx, myeloperoxidase activity and edema formation exhibited by changes in skin thickness which together verify inflammation observed after exposure. The obtained data provide insight into potential mechanisms of dermal toxicity induced by exposure to unpurified SWCNT.

2. Materials and methods

2.1. Chemicals

Fatty acid-free human serum albumin (hSA), luminol, sodium dodecyl sulfate (SDS), glutathione, α-tocopherol were purchased from Sigma Chemicals Co. (St. Louis, MO). Methanol, ethanol, chloroform, hexane and water (HPLC grade) were purchased from Aldrich Chemical Co. (Milwaukee, WI). Thio-Glo-1 was obtained from Covalent Inc. (Wobum, MA). Phosphate buffered saline (PBS) was purchased from Invitrogen Corporation (Carlsbad, CA).

2.2. Particles

SWCNT (CNI, Houston, TX) were produced by the high pressure CO disproportionation process (HiPco) technique (Scott et al., 2003), employing CO in a continuous-flow gas phase as the carbon feedstock and $Fe(CO)_5$ as the iron-containing catalyst precursor. SWCNT were purified by acid treatment to remove metal contaminates (Gorelik et al., 2000). Partially purified SWCNT were comprised of 99.7% (wt) elemental carbon and 0.23% (wt) iron, while unpurified SWCNT contained 30% (wt) iron. We assessed endotoxin content in SWCNT samples used in this study. Level of LPS present in SWCNT samples were evaluated using the Limulus amebocyte lysate (LAL) enzyme assay (DataChem Inc, Salt Lake City, UT). The endotoxin content of SWCNT suspensions was lower than 0.11 EU/ml.

2.3. JB6 P+ cell culture

Epidermal JB6 P+ cells were used to study effects of SWCNT on the AP-1 and NFκB pathways involved in mediating inflammatory responses (Dhar et al., 2002; Colburn et al., 1979; Colburn and Lockyer, 1982). The JB6 family of mouse epidermal clonal genetic variants (P^+/P^-) provides a suitable model for studying critical gene regulation events. Tumor-promotion sensitive JB6 P+ cells respond irreversibly to phorbol esters resulting in the induction of anchorage independent growth as well as tumorgenicity (Dhar et al., 2002; Colburn et al., 1979; Colburn and Lockyer, 1982). JB6 P+ mouse epidermal cells are transfected with an AP-1-luciferase reporter plasmid (JB6/AP-1) or a NFKβ luciferase reporter plasmid (JB6/NFKβ). The cell line was a kind gift from the laboratory of Dr. Nancy Colburn (National Institutes of Health, Frederick, MD). The JB6 P+ cells were cultured in Eagle's MEM containing 5% fetal bovine serum and 2 mM L-glutamine. The cells were grown at 37 °C in a 5% CO_2 atmosphere to reach 80% confluency prior to exposure to SWCNT.

2.4. ESR determination of SWCNT-induced radical formation

ESR spin trapping technique was used to detect formation of free radicals after SWCNT exposure. Spin-trapped radical adducts of hydroxyl radicals ($OH^•$) were measured using 5,5-dimethyl-1-pyrroline-N-oxide (DMPO; 200 mM) spin-trapping agent as previously reported (Shvedova et al., 2003). All ESR measurements were conducted using a Bruker EMX spectrometer (Bruker Instruments Inc. Billerica, MA 01821, USA) with a flat cell assembly. JB6 cells (1×10^6 cells/ml) were suspended in 1× PBS pH 7.4 and incubated with the spin trap DMPO in the presence/absence of unpurified SWCNT (0.12 mg/ml). Samples were incubated for 5 min in a 37 °C water bath and than transferred to an ESR flat cell for measurement at room temperature with instrument settings of microwave power, 63 mW; modulation amplitude, 1.0G; time constant, 40.96 ms; center field, 3480G; sweep width, 100G.

All spectra shown are the accumulation of five scans. Hyperfine couplings constants were determined using the WinSim program of the NIEHS public EPR software tools, available over the internet (http://epr.niehs.nih.gov). The relative radical concentration was estimated by measuring the peak-to-peak height (mm) of the observed spectra.

2.5. AlamarBlue viability assay

The viability of cells following exposure was determined using the AlamarBlue bioassay (Alamar Biosciences, Inc., Sacramento, CA), as described by Keane et al. (1997). Cells were incubated at 37 °C with 10% AlamarBlue (4 h). A fluorescence multiwell plate reader (CytoFluor Series 4000, Perseptive Biosystems, Framingham, MA) with 530 nm excitation and 580 nm emission was then employed in the assay. The results are analyzed using CytoFluor Version 4.2.1 (PerSeptive Biosystems, Framingham, MA).

2.6. Assay of AP-1 and NFKβ activity in vitro

To study whether SWCNT exposure caused changes in AP-1 and NFκB activities, JB6 P+ cells (5×10^4 cells/ml) were cultured in 96-well plates (200 μl per well) in Eagle's MEM supplemented media with 5% fetal bovine serum plus 2 mM L-glutamine. Plates were incubated at 37 °C in a humidified atmosphere of 5% CO_2. Twelve hours later, cells were then cultured in MEM supplemented media with 0.5% FBS (24 h) to minimize basal AP-1 and NFκB activity after which JB6 P+ cells were exposed to unpurified (30% wt iron) or partially purified (0.23% wt iron) SWCNT or vehicle (PBS). Following 24 h incubation with SWCNT (0.06 mg/ml, 0.12 mg/ml, or 0.24 mg/ml), the cells were incubated with 200 μl of 1× lysis buffer provided by the manufacturer (Promega, Madison, WI), and the luciferase activity was measured using a luminometer (Monolight 2010, Analytical Luminescence Laboratory, San Diego, CA). The results are expressed as relative AP-1 or NFκB activity compared to respective controls.

2.7. SWCNT effects on engineered human skin

The EpiDermFT full thickness normal (non-transformed), human cell-derived, three dimensional, organotypic *in vitro* skin tissue model (MatTek Corporation, Ashland, MA) was used to study morphological changes and release of inflammatory mediators induced by unpurified SWCNT exposure. The EpiDermFT construct consists of an epidermal layer containing normal, human-derived epidermal keratinocytes and a dermal layer consisting of normal human dermal fibroblasts. The layers correspond to normal human skin, and the engineered tissue exhibits *in vivo*-like growth and morphological characteristics. The tissues were cultured in a six-well plate using an air–liquid interface technique. The tissues were grown on a semi-permeable membrane and cultivated on Millicell-CM culture inserts. The surface of the tissue is exposed to air which promotes cell differentiation (Belyakov et al., 2005; Curren et al., 2006). The tissues were fed with serum free media from below and exposed to 75 μg unpurified SWCNT or PBS (150 μl DMEM/phenol free, 18 h). Cell culture medium was collected to assess inflammatory cytokine production following SWCNT exposure. Exposed samples were formalin fixed, paraffin embedded and hematoxylin and eosin stained for histological evaluation.

2.8. Production of cytokines by skin

Levels of the mouse inflammatory cytokines, IL-6, MCP-1, IFN-γ, TNF-α, and IL-12, were assayed in the supernatant of engineered skin and skin homogenates of

SKH-1 mice following SWCNT exposure. The concentrations were determined using the BD Cytometric Bead Array, Mouse Inflammation kit (BD Biosciences, San Diego, CA). Six bead populations with distinct fluorescence intensities have been coated with capture antibodies specific for IL-6, IL-10, MCP-1, IFN-γ, TNF-α, and IL-12p70 proteins. The six bead populations are mixed together to form the BD™ CBA which is resolved in the FL3 channel of a flow cytometer. The sensitivity of the assay is 5–7.3 pg/ml.

2.9. Animals

SKH-1 Hairless mice (3–4 weeks; 16–18 g body weight) were obtained from Charles River Laboratory (Wilmington, MA). Each mouse was housed in an individual ventilated cage with Alpha-Dri cellulose chips and hardwood Beta-chips for bedding and provided HEPA-filtered air under controlled environmental conditions in an Association for Assessment and Accreditation of Laboratory Animal Care (AAALAC) accredited, specific pathogen-free facility. NIH-31 (Teklad 7913) diet and water were provided ad libitum. All animal procedures were performed in accordance with an approved Animal Care and Use Committee (ACUC) protocol.

2.10. Animal exposures

SKH-1 mice were topically exposed to unpurified SWCNT (30% wt iron; 40 μg/mouse, 80 μg/mouse, or 160 μg/mouse in deionized water) daily for 5 days. Twenty-four hours following the last exposure, mice were sacrificed with sodium pentobarbital, and skin was removed for biochemical and histological analysis.

2.11. Skin collections and preparation of homogenates

Following SWCNT exposure, skin flaps from the intrascapular area of the back of mouse were excised, and samples taken for histopathology and biochemical analysis. Skin for biochemical analysis was immediately frozen at −80 °C until further processed. Skin homogenates were prepared from frozen tissues with ice-cold phosphate-buffered saline (PBS, 7.4) using a tissue tearer (model 985–370, Biospec Products, Inc., Racine, WI). Skin for histological analysis was fixed in 10% neutral buffered formalin. After fixation, the tissue samples were embedded and sectioned at 5 μm. Sections were stained with hematoxylin and eosin or 0.1% toluidine blue to evaluate mast cell influx.

2.12. Skin thickness

To assess the extent of SWCNT-induced edema in mouse skin following SWCNT treatments, skin bi-fold thickness was assessed using a dial caliper (The Dyer Company, Lancaster, PA), and changes in epidermal cell thickness and mast cell infux were assessed histologically. Changes in skin bi-fold thickness were determined by the measurements of three random locations within the area of exposure per mouse.

To determine mast cell influx as well as changes in epidermal thickness, cell counts were recorded using a light microscope (Olympus B X 40) with a high objective (40×). Epidermal cell thickness was evaluated in hematoxylin and eosin stained sections, while 0.1% toluidine blue was used to stain sections to evaluate mast cell influx. Ten random fields were examined per slide with cell counts evaluated in both the dermis and epidermis. Cumulative counts from these 10 fields were recorded as the relative number of cells for that sample. Photomicrographs were prepared using an Olympus 300 double-headed microscope (Tokyo, Japan).

2.13. Collagen accumulation in skin of SKH-1 mice exposed to SWCNT

Total collagen content in the skin was determined by quantifying total soluble collagen using the Sircol Collagen Assay kit (Accurate Chemical and Scientific Corporation, Westbury, NY). Briefly, skin homogenates were mixed with 0.5 M acetic acid containing pepsin (Accurate Chemical and Scientific Corporation, Westbury, NY). Each sample was stirred vigorously for 24 h at 4 °C, centrifuged, and 200 μl of supernatant was assayed according to the manufacturer's instructions.

2.14. Myeloperoxidase levels in the skin of SWCNT-exposed mice

Inflammatory response in the skin of SKH-1 mice treated with SWCNT was assessed by measurement of myeloperoxidase (MPO) activity by Enzyme Linked Immunosorbent Assay (ELISA). The concentration of MPO in skin homogenates was measured using a commercially available ELISA immunoassay kit (Cell Sciences, Canton, MA) with detection limit ranging from 1.02 ng/ml to 250 ng/ml. Each measurement of MPO activity in skin homogenates were assayed in duplicate and normalized to total protein content in skin samples.

2.15. Fluorescence assay of glutathione (GSH)

Glutathione concentration in cell and skin homogenates was determined using ThioGlo-1, a maleimide reagent which produces a highly fluorescent product upon its reaction with sulfhydryl groups (Shvedova et al., 2000). A standard curve was established by addition of GSH (0.04–2.0 μM) to 0.1 M phosphate buffer (pH 7.4) containing 10 μM ThioGlo-1. GSH content was estimated by an immediate fluorescence response registered upon addition of ThioGlo-1 to tissue homogenates. A Shimadzu spectrofluorometer RF-5000 U (Shimadzu, Japan) was employed in the assay: excitation 388 nm and emission 500 nm. The data were acquired using an excitation slit of 1.5 nm and an emission slit of 5 nm. The fluorescence signals were exported from the spectrofluorometer using RF-5000 U PC Personal Fluorescence software (Shimadzu, Japan).

2.16. Determination of protein carbonyls in the skin of mice exposed to SWCNT

Oxidation of proteins in the skin homogenates prepared from SKH-1 mice exposed to SWCNT were evaluated by measurement of protein carbonyls using ELISA (Northwest Life Sciences, Vancouver, WA). Briefly, protein was extracted from homogenates according to manufacturer's instructions. Protein extracts were then incubated with dinitrophenylhydrazine (DNP) and assayed colorimetrically at 450 nm. The assay provides detection limits of protein carbonyl within 0.10–0.93 nmol/mg protein. Each sample of skin homogenate was assayed in duplicate.

2.17. Protein assay

Measurements of protein in homogenates from mouse skin were run using a Bio-Rad protein assay kit, catalog no. 500–0006 (Richmond, CA).

2.18. Statistics

Treatment related differences were evaluated using two-way ANOVA, followed by pair-wise comparison using the Student–Newman–Keuls tests, as appropriate. Statistical significance was considered at $p < 0.05$.

3. Results

3.1. ESR detection of SWCNT-induced free radicals in JB6 P+ cells

The ESR spin trapping technique was used to detect free radical generation during incubation of SWCNT with JB6 P+ cells. Fig. 1 shows the ESR spectra of a typical DMPO spin-trapped OH• radical at different time points after exposure to SWCNT. This spectrum consists of a 1:2:2:1 quartet with splittings of $a^H = a^N = 14.9$ G, where a^H and a^N denote hyperfine splittings of the α-hydrogen and the nitroxyl nitrogen, respectively. On the basis of these coupling constants, the 1:2:2:1 quartet was assigned to DMPO/•OH adduct. Addition of H_2O_2 dramatically increased the DMPO/•OH adduct signal (Fig. 2B), while addition of catalase, an H_2O_2 scavenger, to the incubation system decreased the generation of •OH radical (Fig. 2C). Addition of the metal chelator, deferoxamine (DFO), also strongly

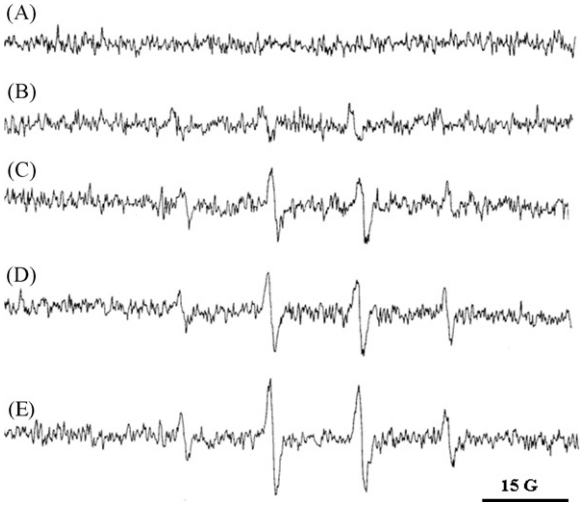

Fig. 1. Formation of free radicals from SWCNT-stimulated JB6 P+ Cells. Electron spin resonance (ESR) spectrum recorded for 15 min after the addition of SWCNT (0.12 mg/ml) to JB6 P+ (10^6 cells/ml) in PBS (pH 7.4) containing 40 mM 5,5-dimethyl-1-pyrroline-1-oxide. (A) 0 min, (B) 1 min, (C) 5 min, (D) 10 min and (E) 15 min. Instrumental conditions: microwave power, 50 mW; modulation amplitude, 1.0G; time constant, 40.96 ms; center field, 3435G; sweep width, 100G.

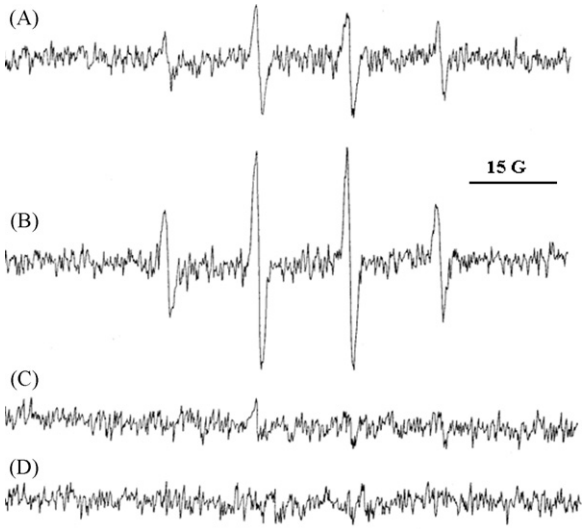

Fig. 2. Generation of free radicals from SWCNT-stimulated JB6 P+ cells. (A) Electron spin resonance (ESR) spectrum recorded 5 min after the addition of SWCNT (0.12 mg/ml) to JB6 P+ (10^6 cells/ml) in a phosphate-buffered solution (pH 7.4) containing 200 mM 5,5-dimethyl-1-pyrroline-1-oxide. (B) Same as A plus 1 mM H_2O_2 added. (C) Same as A plus 20 U/ml catalase added. (D) Same as A plus 0.2 mM deferoxamine added. Instrumental conditions: microwave power, 63 mW; modulation amplitude, 1.0G; time constant, 40.96 ms; center field, 3480G; sweep width, 100G.

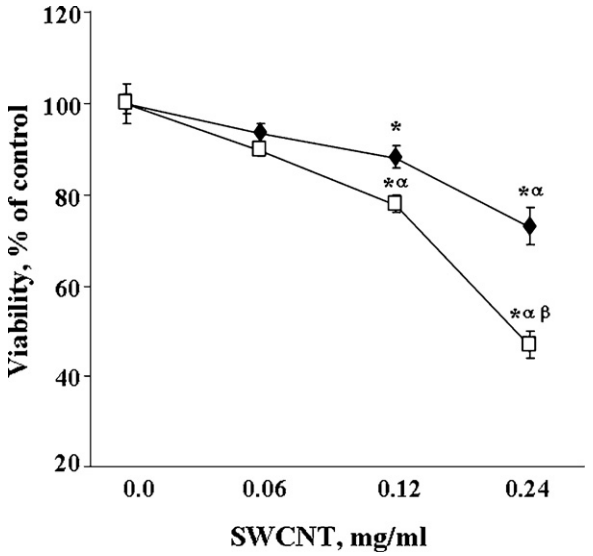

Fig. 3. Viability of JB6 P+ cells following exposure to SWCNT. Conditions: JB6 P+ cells (1×10^6) were incubated in phenol-free MEM in the absence and in the presence of 0.06 mg/ml, 0.12 mg/ml, or 0.24 mg/ml partially purified (black diamonds) or unpurified (white squares) SWCNT for 24 h at 37 °C. After the incubation, cells were washed twice with PBS (pH 7.4) and then cell viability was determined with 10% AlamarBlue. Values are means ± S.E.M. of three experiments. Significance indicated by: $^*p < 0.05$ versus control; $^\alpha p < 0.05$ versus 0.06 mg/ml SWCNT; $^\beta p < 0.05$ versus 0.12 mg/ml SWCNT.

suppressed the DMPO/•OH signal (Fig. 2D). These results suggested that •OH generated during exposure of SWCNT to JB6 P+ cells was formed via a metal-dependent Fenton reaction.

3.2. Effect of SWCNT on cell viability, oxidative stress and cytokine release in JB6 cells

The AlamarBlue assay demonstrated a significant concentration-dependent decrease in viability following exposure of JB6 P+ cells to both partially purified and unpurified SWCNT. Partially purified SWCNT resulted in a dose-dependent decrease in viability – 6.6% (0.06 mg/ml), 11.9% (0.12 mg/ml), and 27.7% (0.24 mg/ml) – after exposure to SWCNT (24 h) (Fig. 3). A more profound decrease in viability (10.2% at 0.06 mg/ml, 22.1% at 0.12 mg/ml, and 53.07% at 0.24 mg/ml) occurred following exposure of JB6 P+ cells to unpurified SWCNT (Fig. 3).

Nonprotein thiol levels in JB6 P+ cells were evaluated to assess SWCNT-induced oxidative stress using a maleimide SH-reagent, ThioGlo-1 (Kagan et al., 1999; Shvedova et al., 2000). A significant dose-dependent decrease of GSH was observed with decreases of 19%, 25.9%, and 47.95% after incubation (24 h) of JB6 P+ cells with 0.06 mg/ml, 0.12 mg/ml, and 0.24 mg/ml partially purified SWCNT, respectively (Fig. 4). Exposure to unpurified SWCNT induced a more profound reduction in GSH than was observed following exposure to partially purified SWCNT (Fig. 4). Reductions GSH of 50%, 54.2%, and 66.7% were observed after 24 h incubation of JB6 P+ cells with 0.06 mg/ml, 0.12 mg/ml, or 0.24 mg/ml unpurified SWCNT, respectively.

3.3. Activation of AP-1 in JB6 P+ following exposure to SWCNT

Activation of AP-1 was assessed in JB6 P+ cells exposed to partially purified and unpurified SWCNT (24 h). Exposure of JB6 P+ cells to 0.06 mg/ml, 0.12 mg/ml, or 0.24 mg/ml unpurified SWCNT caused a dose-dependent increase of 15%, 50%, and 92% in AP-1 activity following exposure. Partially purified SWCNT did not significantly induce activation of AP-1 (Fig. 5).

3.4. Activation of NFκB in JB6 P+ cells after exposure to SWCNT

NFkB is a redox-sensitive transcription factor which is involved in the regulation of a number of inflammatory reactions (Driscoll et al., 1997; Mossman and Churg, 1998; Schins and Borm, 1999). We found that exposure to unpurified SWCNT caused a significant dose-dependent (44%, 50%, and 76%) induction of NFkB when cells were treated with 0.06 mg/ml, 0.12 mg/ml, and 0.24 mg/ml SWCNT, respectively. A similar activation of NFkB was also observed when the cells were exposed to partially purified SWCNT. Both unpurified and partially purified SWCNT had similar effects in NFkB activation (76% and 80%) after exposure of JB6 P+ cells to 0.24 mg/ml SWCNT for 24 h (Fig. 6).

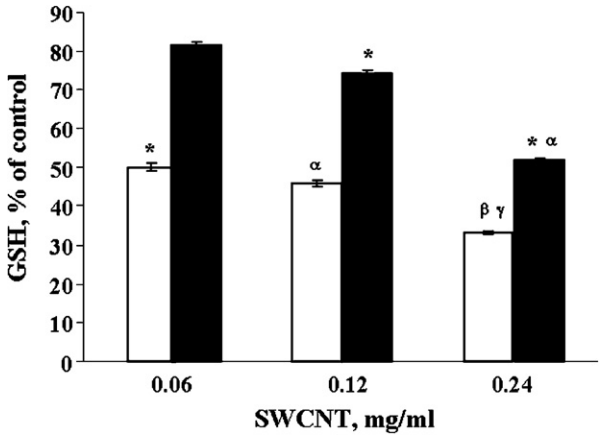

Fig. 4. Glutathione (GSH) Depletion in JB6 P+ cells following exposure to SWCNT. Conditions: JB6 P+ cells (1×10^6) were incubated in phenol-free MEM in the absence and in the presence of 0.06 mg/ml, 0.12 mg/ml, or 0.24 mg/ml unpurified (white bars) or partially purified (black bars). SWCNT for 24 h at 37 °C. After the incubation, cells were washed twice with PBS (pH 7.4) and GSH levels were determined. Values are means ± S.E.M. of three experiments. $^*p < 0.05$ versus 0.06 mg/ml partially purified SWCNT; $^\alpha p < 0.05$ versus 0.12 mg/ml partially purified SWCNT; $^\beta p < 0.05$ versus 0.24 mg/ml partially purified SWCNT; $^\gamma p < 0.05$ versus 0.06 mg/ml unpurified SWCNT.

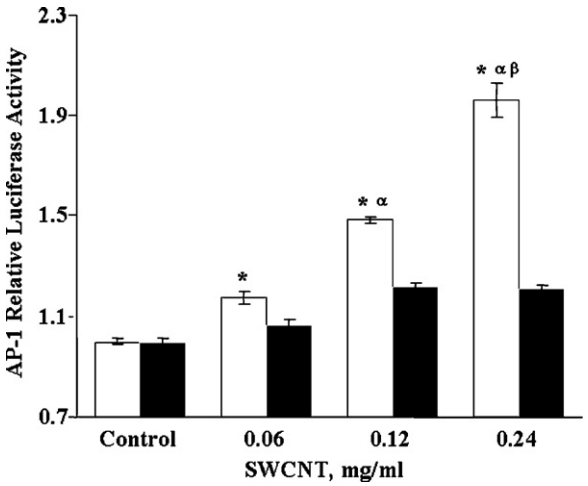

Fig. 5. SWCNT-induced activation of AP-1 in JB6 P+ cells. JB6 P+ cells transfected with an AP-1 luciferase reporter plasmid were exposed to unpurified (white bars) or partially purified SWCNT (black bars). Twenty-four hours following exposure, cells were extracted with 200 μl of 1× lysis buffer provided in luciferase assay kit and the luciferase activity was measured using a luminometer. The results are expressed as relative AP-1 activity compared to respective controls. Values are means ± S.E.M. of three experiments. $^{*}p < 0.05$ versus control; $^{\alpha}p < 0.05$ versus 0.06 mg/ml SWCNT; $^{\beta}p < 0.05$ versus 0.12 mg/ml SWCNT.

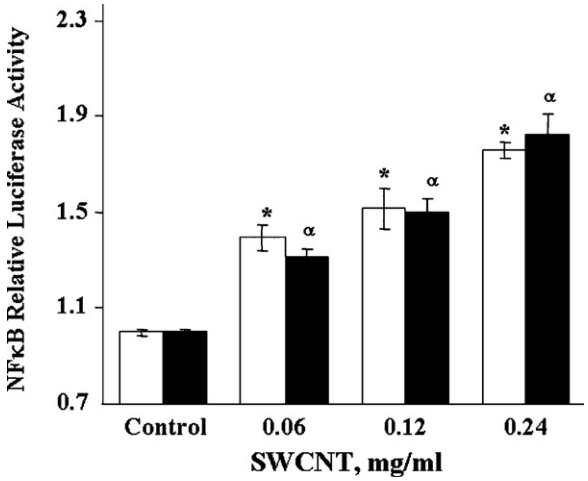

Fig. 6. SWCNT-induced activation of NFκB in JB6 P+ cells (24 h). JB6 P+ cells transfected with an NFκB luciferase reporter plasmid were exposed to unpurified (white bars) or partially purified SWCNT (black bars). Twenty-four hours following exposure, cells were extracted with 200 μl of 1× lysis buffer provided in luciferase assay kit and the luciferase activity was measured using a luminometer. The results are expressed as relative NFκB activity compared to respective controls. Values are means ± S.E.M. of three experiments. $^{*}p < 0.05$ versus unpurified control; $^{\alpha}p < 0.05$ versus partially purified control.

3.5. Effect of unpurified SWCNT on engineered human skin

EpidermFT, a normal human cell-derived *in vitro* skin tissue model, was used to evaluate morphological changes of the skin induced by exposure to unpurified SWCNT. Histopathology of EpidermFT engineered skin revealed an accumulation of fibroblasts and basal squamous cells of the epidermis after exposure to unpurified SWCNT, while no changes were observed in the control skin sections exposed to vehicle. Parakeratosis and hyperkeratosis are evident. Evaluation of Sirius red stained sections revealed an increase amount of collagen in the SWCNT-exposed engineered skin (data not shown). The thickness of the dermis of the unpurified SWCNT-exposed engineered skin was 1.5-fold greater compared to those in control skin sections (Fig. 7A and B).

3.6. Cytokine production by engineered skin following unpurified SWCNT exposure

Exposure of EpidermFT to unpurified SWCNT induced the release of a number of inflammatory cytokines. IL-6, IL-12, and IFN-γ were all significantly elevated following exposure to unpu-

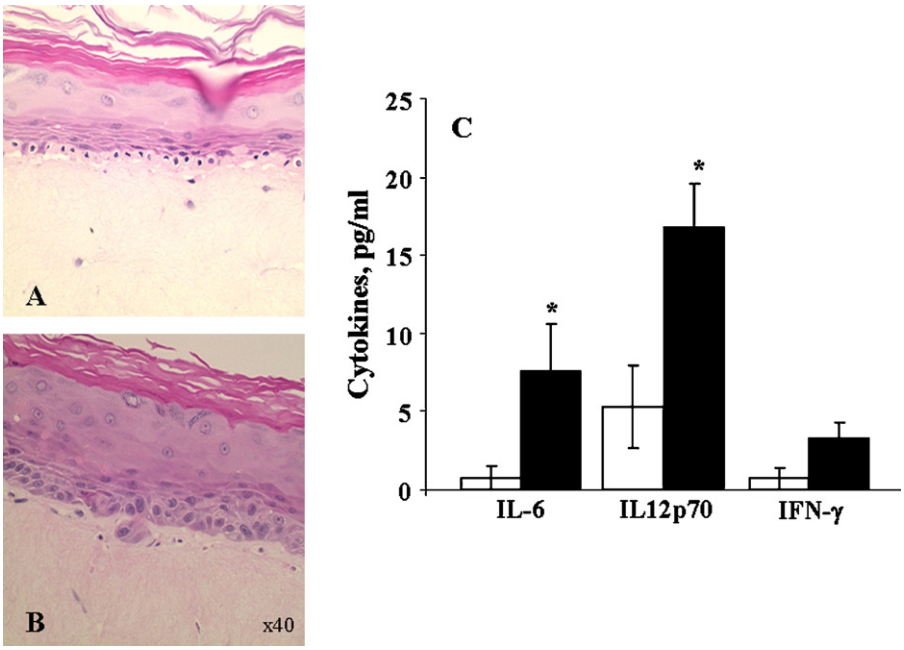

Fig. 7. SWCNT-induced alterations to engineered human skin. (A and B) Photomicrographs of engineered skin sections following exposure to PBS (A) or unpurified SWCNT (B). (C) Cytokine release from engineered skin in response to unpurified SWCNT exposure. White bars, PBS exposed; black bars, unpurified SWCNT exposed. EpiDerm FT skin tissue model was exposed to 75 μg of unpurified SWCNT for 18 h. Following exposure, samples were formalin fixed, paraffin embedded and stained with hematoxylin and eosin to evaluate morphological alterations. $^{*}p < 0.05$ versus PBS-exposed control mice.

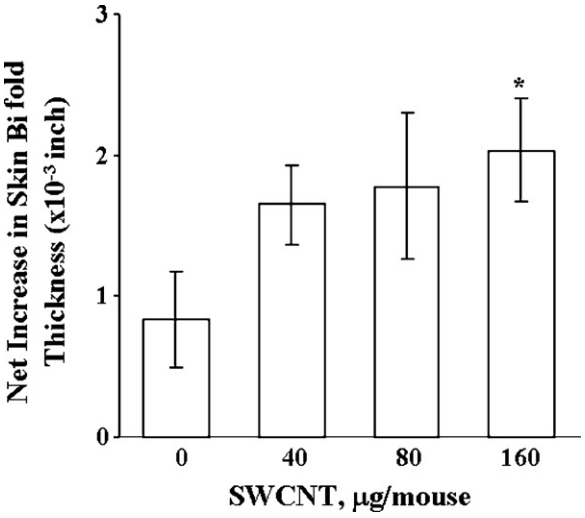

Fig. 8. Net increase in skin bi-fold thickness of SKH-1 Mice topically treated with unpurified SWCNT for 5 days. SKH-1 mice were topically exposed to unpurified SWCNT (30% weight iron; 40 μg/mouse, 80 μg/mouse, or 160 μg/mouse) daily for 5 days. Twenty-four hours following the last exposure, mice were sacrificed. Values are means ± S.E.M. of three experiments. *$p < 0.05$ versus PBS-exposed control mice.

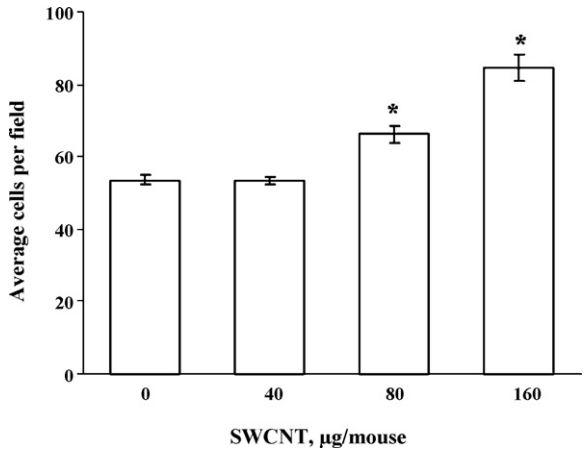

Fig. 9. Epidermal cell number of SKH-1 mice dermally exposed to unpurified SWCNT. SKH-1 mice were topically exposed to unpurified SWCNT (30% weight iron; 40 μg/mouse, 80 μg/mouse, or 160 μg/mouse) daily for 5 days. Twenty-four hours following the last exposure, mice were sacrificed. Values are means ± S.E.M. of three experiments. *$p < 0.05$ versus vehicle control.

rified SWCNT. SWCNT exposure had the most profound effect on IL-6 (increased 14 times). In addition, IFN-γ and IL-12 were also significantly increased by 7 and 2.5 times, respectively (Fig. 7C). TNF-α and MCP-1 levels were not significantly elevated following exposure to unpurified SWCNT (data not shown).

3.7. Inflammation and histopathology of the skin of SKH-1 mice exposed to unpurified SWCNT

Topical exposure to unpurified SWCNT induced an increase in skin thickness of SKH-1 mice following exposure to 40 μg/mouse, 80 μg/mouse, or 160 μg/mouse for 5 days and observed 1 day post-treatment. Skin bi-fold thickness as well as cell numbers within the epidermis and dermis were assessed pre- and post-mortem, respectively. Skin bi-fold thickness was measured daily and used as an indicator of edema and skin inflammation. Topical treatment with unpurified SWCNT (160 μg/mouse) resulted in significant increase in skin bi-fold thickness (150%) assessed following 5 days exposure as compared to those in control mice (Fig. 8). No changes in skin thickness were observed at time-points prior to 5 days of exposure (data not shown).

Changes in the number of cells present within the skin of SKH-1 mice following unpurified SWCNT exposure were quantified within the epidermis and compared to the control group. Counts of cells within the epidermis of animals exposed to 80 μg/mouse and 160 μg/mouse SWCNT revealed a 25% and 58% increase in the amount of cells within the epidermis, respectively (Fig. 9). Exposure to 40 μg/mouse and 80 μg/mouse did not reveal any significant increase in mast cell accumulation (data not shown) within the dermis, while the highest dose of unpurified SWCNT (160 μg/mouse) caused a 90% increase in mast cells influx observed in the skin of SKH-1 mice (Fig. 10A).

Another marker of skin injury, myeloperoxidase (MPO), was measured to determine the inflammatory response to unpurified SWCNT. MPO, a well-recognized marker of neutrophil influx into tissue, was increased after topical exposure to unpurified SWCNT. We found that low doses of unpurified SWCNT (40 μg/mouse and 80 μg/mouse) did not induce any changes in MPO activity in skin of exposed mice. Topical treatment with 160 μg/mouse of unpurified SWCNT was found to cause a 21% increase in MPO activity (Fig. 10B).

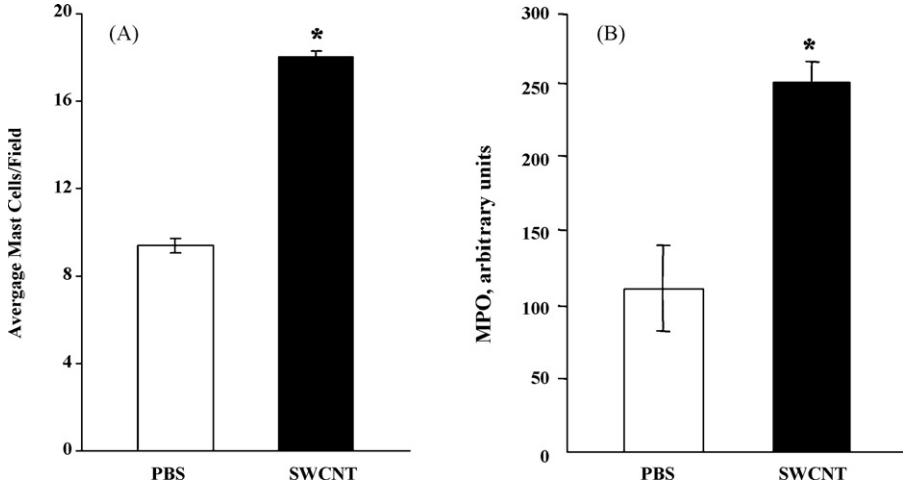

Fig. 10. Mast cell infiltration (A) and myeloperoxidase activity (B) in skin of SKH-1 mice topically exposed to unpurified SWCNT. SKH-1 mice were topically exposed to unpurified SWCNT (30% weight iron; 160 μg/mouse) daily for 5 days. Twenty-four hours following the last exposure, mice were sacrificed with sodium pentobarbital, and skin was removed frozen for biochemical analysis. Values are means ± S.E.M. of three experiments. *$p < 0.05$ versus PBS.

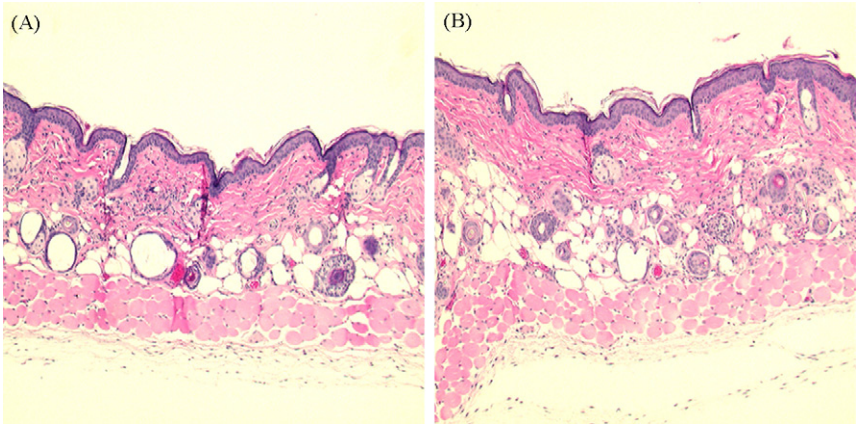

Fig. 11. Skin photomicrographs of SKH-1 mice topically treated with unpurified SWCNT. (A) Control (PBS) exposed mice; (B) unpurified SWCNT (160 μg/mouse) exposed mice. SKH-1 mice were topically exposed to unpurified SWCNT (30% weight iron; 160 μg/mouse) daily for 5 days. Twenty-four hours following the last exposure, mice were sacrificed with sodium pentobarbital and skin was removed and fixed in formalin for histological analysis. Values are means ± S.E.M. of three experiments.

Histological evaluation of the skin of unpurified SWCNT-exposed (160 μg/mouse) mice revealed accumulation of polymorphonuclear leukocytes (PMNs) within the epidermis and dermis as compared to control-exposed skin (Fig. 11A). The inflammation, i.e. recruitment of PMNs, was localized around or within the hair follicles. Increased inflammation was observed in adipose tissue as well as a few sebaceous glands of SWCNT-exposed mice. Also, the skin of mice exposed to unpurified SWCNT showed increased mast cell activity and degranulation that was not observed in the skin of control mice (Fig. 11B).

3.8. Collagen accumulation in skin of SKH-1 mice dermally exposed to unpurified SWCNT

Exposure of SKH-1 mouse skin to unpurified SWCNT resulted in increased collagen accumulation. The highest dose of unpurified SWCNT (160 μg/mouse) induced a significant 12% increase in collagen found in the skin (Fig. 12A). The lower doses of unpurified SWCNT (40 μg/mouse and 80 μg/mouse) did not significantly change the amount of collagen present in the skin as compared to control (data not shown).

3.9. Oxidative damage in skin of SKH-1 mice following unpurified SWCNT exposure

To assess whether unpurified SWCNT induced oxidative stress, we measured changes in antioxidant levels, and protein oxidation. After unpurified SWCNT exposure, we found that the highest dose (160 μg/mouse) induced a significant 11% reduction in GSH in the skin (Fig. 12B). We observed no changes in GSH in the skin of mice exposed to 40 and 80 μg/mouse of unpurified SWCNT (data not shown).

Protein oxidation, assessed by measurements of carbonyl formation in mouse skin, did not significantly differ in the skin of mice exposed to the lowest dose of unpurified SWCNT (40 μg/mouse). However, exposure to 80 μg/mouse and 160 μg/mouse of unpurified SWCNT resulted in a significant 34% and 41% increase in carbonyl content found in the skin of exposed mice as compared to control (Fig. 13).

3.10. Cytokine production in the skin of SKH-1 mice exposed to unpurified SWCNT

Inflammatory cytokines, e.g. IL-6, IL-10, MCP-1, IFN-γ, TNF-α, and IL-12p70, were evaluated in the supernatant of skin homogenates from SKH-1 mice following exposure to unpurified SWCNT. SKH-1 mice exposed to 40 μg/mouse and 80 μg/mouse of unpurified SWCNT showed no increase in cytokine release (data not shown). The highest dose of unpurified SWCNT (160 μg/mouse) induced a significant release of IL-10 and IL-6 (100% and 80%, respectively) in the skin (Fig. 14). No changes were observed in MCP-1, IFN-γ, TNF-α, and IL-12 at the highest dose of unpurified SWCNT (data not shown).

4. Discussion

Single wall carbon nanotubes are a newly developed allotrope of carbon with extraordinary mechanical and electrical properties which offer possibilities for the development of new nanoelectronics devices, circuits, and computers. A previous study characterizing SWCNT aerosol formation during laboratory usage revealed a high potential for dermal exposure (Maynard et al., 2004). Air samples showed a concentration of SWCNT between 0.70 $\mu g/m^3$ and 53 $\mu g/m^3$; however, more revealing was the concentration present on individual gloves of laboratory workers which ranged from 217 μg to 6020 μg (Maynard et al., 2004). Dermal exposure to carbon materials has been shown to result in the development of a variety of skin disorders, i.e. carbon fiber dermatitis, hyperkeratosis, and nevi (Lachapelle, 2002; Eedy, 1996; Jenkinson, 1997; NIOSH, 1978; Kasparov et al., 1989). However, the unique properties of SWCNT may also result in the unusual development of skin disorders (Borm, 2002).

Manufacturing of SWCNT relies heavily on the use of catalytic metals. Transition metals, e.g. iron, cobalt and nickel, are known to induce formation of reactive oxygen species (ROS) and subsequently cause oxidative stress (Kaur et al., 2004; Eisen et al., 2004; Chachami et al., 2004). In this study, we used HiPco materials which are produced utilizing iron as the catalytic metal. The resulting SWCNT contains iron which is encased in a carbon shell and distributed throughout the nanotube (Chiang et al., 2001). Iron exposure poses a minimal health risk with no adverse health effects occurring from skin contact (Lepinski and Myers, 1995). Currently, iron compounds are widely used as colorants in a number of cosmetic products which are applied to the skin, hair, and nails (Lansdown, 2001). Iron overload toxicity is associated with the development of free-radical mediated tissue damage, which may result in the development and progression of a number of pathological conditions (Cavaleri and Rogan, 1992; Rockey, 2003; Bing, 2001; Maritim et al., 2003; Ahsan et al., 2003; Fraga and Oteiza, 2002). A previous study found that SWCNT-associated iron can catalyze the decomposition of hydrogen peroxide and organic peroxides thus forming a hydroxyl radical from hydrogen peroxide or

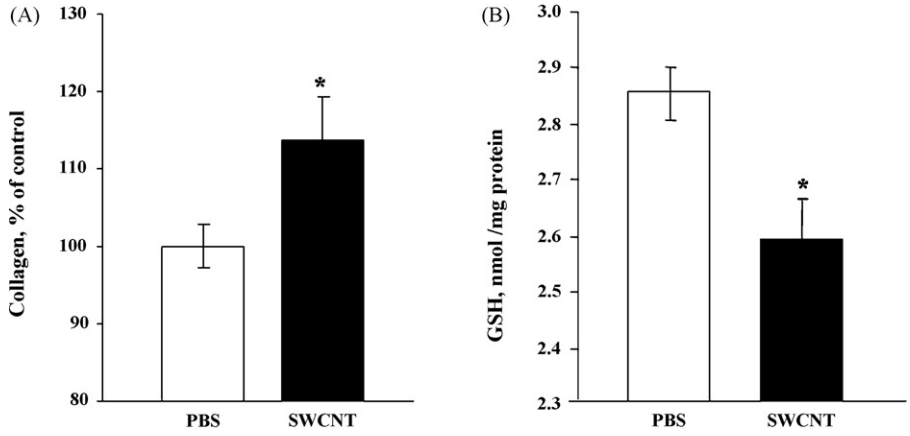

Fig. 12. Collagen accumulation (A) and glutathione depletion (B) in skin of SKH-1 mice topically treated with unpurified SWCNT for 5 days. SKH-1 mice were topically exposed to unpurified SWCNT (30% weight iron; 160 μg/mouse) daily for 5 days. Twenty-four hours following the last exposure, mice were sacrificed with sodium pentobarbital, and skin was removed frozen for biochemical analysis. Values are means ± S.E.M. of three experiments. $^{*}p < 0.05$ versus PBS-exposed control mice.

alkoxyl radicals from lipid peroxide (Shvedova et al., 2003). Exposure of JB6 P+ cells to unpurified SWCNT resulted in the formation of ESR detectable hydroxyl radicals. Incubation of JB6 P+ cells with SWCNT in the presence of DFO (metal/iron chelator), reduced radical formation thereby providing evidence that the observed ROS formation was induced via a metal-dependent Fenton reaction.

Reactive oxygen species (ROS) are capable of modifying the activity of proteins on the post-translational level and regulating gene expression (Sies, 1991; Meyer et al., 1994). AP-1 and NFkB are two important transcriptional factors which have been shown to be regulated by changes in the redox state of the cell in part due to overproduction of ROS (Meyer et al., 1994; Abate and Curran, 1990; Toledano and Leonard, 1991). AP-1 activation occurs from the upregulation of protein kinase C in response to oxidant exposure (Boyle et al., 1991; Papavassiliou et al., 1992; Cerruti, 1989), while activation of NFkB occurs due to ROS acting as a second messenger (Schreck et al., 1991; Schreck and Baeuerle, 1991). In the case of SWCNT exposure, unpurified SWCNT resulted in the induction of both NFkB and AP-1, while partially purified SWCNT only induced NFkB. Hydrogen peroxide exposure has been found to be a more effective inducer of NFkB than AP-1 (Meyer et al., 1994) indicating that NFkB may be more sensitive to redox changes within the cell or tissue (Meyer et al., 1994).

Upregulation of NFkB and AP-1 has been shown to increase production of a number of cytokines and chemokines, including IL-1, IL-6, IL-8, TNF-α, MCP-1, MIP-1α, MIP-2, COX-2 and iNOS, which are responsible for the development of a number of disease states (Driscoll et al., 1997; Mossman and Churg, 1998; Schins and Borm, 1999). IL-8, IL-6, and IL-1β have been implicated in the development of dermal irritation (Barker et al., 1991; Corsini and Galli, 1998; Grone, 2002; Nickolof, 1991). Keratinocytes release TNF-α and IL-1β in response to acute tissue injury or inflammation. Release of IL-8, which plays a role in skin inflammatory disease (Chabot-Fletcher et al., 1994), is stimulated by TNF-α and IL-1β. Exposure of human epidermal keratinocytes (NEK) to multiwalled carbon nanotubes has been shown to induce the release of IL-8, a marker of dermal irritation in humans (Monteiro-Riviere et al., 2005). Additionally, exposure of NEKs to amino acid-functionalized fullerenes, an allotrope of carbon, induced the release of IL-1β and IL-6 (Rouse et al., 2006). In our experiments, exposure of engineered skin to unpurified SWCNT induced inflammation accompanied by the release of IL-6 and IL-12. IL-6 has been shown to be a major pro-inflammatory mediator produced by keratinocytes in response to

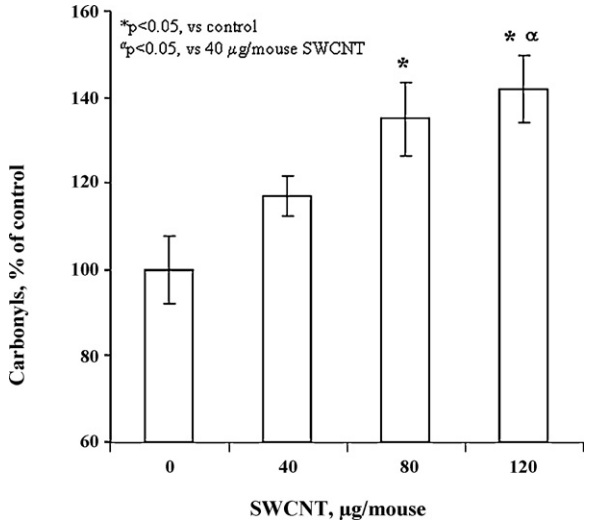

Fig. 13. Protein carbonyls in skin of SKH-1 mice topically treated with unpurified SWCNT for 5 days. SKH-1 mice were topically exposed to unpurified SWCNT (30% wt iron; 40 μg/mouse, 80 μg/mouse, or 160 μg/mouse) daily for 5 days. Twenty-four hours following the last exposure, mice were sacrificed with sodium pentobarbital, and skin was removed frozen for biochemical analysis. Values are means ± S.E.M. of three experiments. $^{*}p < 0.05$ versus PBS-exposed control mice; $^{\alpha}p < 0.05$ versus 40 μg/mouse SWCNT-exposed mice.

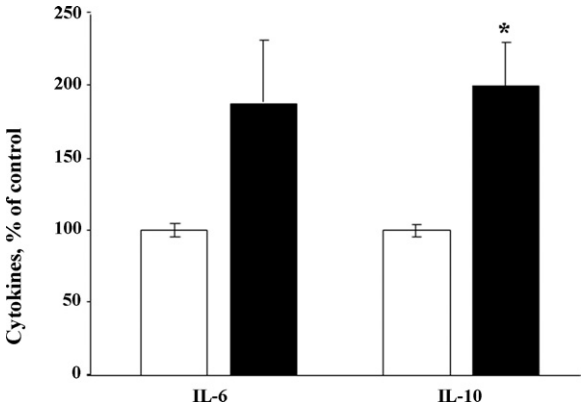

Fig. 14. Cytokine release by SKH-1 mouse skin following dermal exposure to unpurified SWCNT. Open bars, PBS-exposed mice; black bars, SWCNT-exposed mice. SKH-1 mice were topically exposed to unpurified SWCNT (30% wt iron; 160 μg/mouse) daily for 5 days. Twenty-four hours following the last exposure, mice were sacrificed with sodium pentobarbital, and skin was removed frozen for biochemical analysis. Values are means ± S.E.M. of three experiments. $^{*}p < 0.05$ versus PBS.

skin irritants, contact allergens, viruses, UV radiation and thermal damage (Sugawara et al., 2001). Mice dermally exposed to unpurified SWCNT showed increased levels of IL-6 and IL-10 in the skin as well as an influx of mast cells into the tissue. Mast cells have been shown to produce IL-10 (Enk et al., 1994; Chung, 2001). Studies have also shown that the presence of TGF-β and IL-6 can lead to the transformation of naïve T cells into T helper cells, Th17 cells (Bettelli et al., 2006; Veldhoen et al., 2006; McGeachy and Cua, 2008; Li and Flavell, 2008). Th17 cells, which have been stimulated with IL-6 and TGF-β, are capable of secreting IL-10 (McGeachy et al., 2007; Stumhofer et al., 2007). The resulting IL-10 production is believed to regulate Th17 cell immunopathology and result in decreased disease severity (McGeachy et al., 2007). These studies are in agreement with the current data showing that unpurified SWCNT induced the release of a number of inflammatory cytokines, e.g. IL-6 and IL-12, in engineered skin and IL-10 and IL-6 in mouse skin, following exposure.

One of the major goals of our study was to assess whether topical exposure to unpurified SWCNT caused oxidative stress and inflammation. Antioxidants prevent the uncontrolled formation of free radicals, and ROS production in different environmental and occupational exposures, e.g. ozone, ambient particles, diesel, metal working fluids, and ultraviolet radiation (Fuchs et al., 1989; Nishi et al., 1991; Halliwell and Cross, 1994; Tyrrell, 1994; Evelson et al., 1997; Thiele et al., 1997; Podda et al., 1998; Lopez-Torres et al., 1998). Antioxidants are able to regulate ROS production thus protecting biological constituents from accelerated oxidative stress (Chaudiere and Ferrari-Iliou, 1999). Overproduction of ROS could burden the antioxidant capacity of skin thus reducing the skin's ability to withstand oxidative damage. Topical exposure of mice to unpurified SWCNT was found to induce oxidative stress by causing a depletion of GSH, and diminishing of the total antioxidant reserve resulting in an increase in lipid and protein oxidation and inflammation. We found that topical exposure of SKH-1 hairless mice to unpurified SWCNT caused an inflammatory response in the skin as assessed by PMN and mast cell influx, increased MPO activity, as well as increases in skin thickness and edema formation. We could speculate that the inflammatory reaction and oxidative stress detected in skin were mediated via the activation of two redox-sensitive pathways, AP-1 and NFkB, known to regulate a number of inflammatory outcomes taking place in different tissues including skin (Murray et al., 2007; Shvedova et al., 2003; Haddad and Land, 2000; Haddad et al., 2000; Haddad and Harb, 2005).

An important aspect to consider is whether the dermal toxicity of nanoparticles correlates with their ability to penetrate through stratum corneum. Several reports have shown that nano- and micronized particles, e.g. titanium dioxide and beryllium, are able to pass the stratum corneum by translocation via hair follicles (Lademann et al., 1999; Tan et al., 1996; Alvarez-Roman et al., 2004) or an intracellular transcutaneous pathway (Van den Bergh et al., 1999; Honeywell-Nguyen et al., 2004) thus resulting in deposition of particles in the epidermis and/or dermis (Tinkle et al., 2003; Baroli et al., 2007). Tinkle et al. (2003) found that beryllium penetration which occurred by a simple flexing motion was sufficient to induce cutaneous sensitization. However, Ryman-Rasmussen et al. (2006) found that nanosized quantum dots are able to penetrate the stratum corneum barrier without abrasion or mechanical stress. Nanoparticles ranging in size from 7 nm to 20 nm have been shown to have a preference for accumulating in follicular openings (Alvarez-Roman et al., 2004; Schaefer et al., 1990; Lauer et al., 1996; Toll et al., 2004; Meidan et al., 2005; Vogt et al., 2006). In the current study, histological evaluation of the skin of SKH-1 mice exposed to unpurified SWCNT showed inflammation localized around the hair follicles indicating some SWCNT may be able to penetrate the stratum corneum; however, we did not evaluate whether topical exposure of SKH-1 mice to unpurified SWCNT caused penetration and deposition of nanotubes within skin compartments. Despite their small diameter (1–4 nm), SWCNT are quite long and not fully dispersed. The particles utilized in this study were comprised not only of dispersed particles (80%) but also contained aggregated forms (20%). Therefore, it is hard to predict whether the SWCNT used in the current study would be able to efficiently penetrate the stratum corneum. Further research is necessary to determine whether SWCNT and other nano-carbonaceous particles are able to efficiently penetrate via skin thus causing dermal toxicity.

The current results document SWCNT-induced oxidative stress and associated inflammation with the involvement of the activation of the redox sensitive signal transduction pathways, AP-1 and NFκB. Exposure of bioengineered human skin to unpurified SWCNT increased epidermal thickness and accumulation and probable activation of dermal fibroblasts which can result in increased collagen as well as the observed release of pro-inflammatory cytokines. *In vitro* exposure to SWCNT, specifically unpurified SWCNT (30%, w/w iron), caused hydroxyl radical generation, a higher degree of cytotoxicity; unpurified SWCNT were capable of inducing AP-1 and NFkB to a greater extent than partially purified SWCNT which only induced activation of NFkB. *In vivo* dermal exposure to unpurified SWCNT resulted in the development of inflammation and oxidative stress, specifically depletion of glutathione and formation of protein carbonyls. Unpurified SWCNT also induced inflammation in the skin as observed by increased skin thickness, accumulation of PMNs and mast cells, release of MPO and pro-inflammatory cytokines. In conclusion, our data indicate that topical exposure to unpurified SWCNT can cause dermal toxicity associated with free radical generation, oxidative stress, and inflammation.

Conflict of interest

None declared.

Acknowledgements

Supported by NIOSH OH008282, NIH HL70755, NORA 927000Y, NORA 927Z1LU and the 7th Framework Program of the European Commission (EC-FP-7-NANOMMUNE-214281).

References

Abate, C., Curran, T., 1990. Encounters with Fos and Jun on the road to AP-1. Semin. Cancer Biol. 1, 19–26.
Ahsan, H., Ali, A., Ali, R., 2003. Oxygen free radicals and systemic autoimmunity. Clin. Exp. Immunol. 131, 389–404.
Alvarez-Roman, R., Naik, A., Kalia, Y.N., Guy, R.H., Fessi, H., 2004. Skin penetration and distribution of polymeric nanoparticles. J. Control Release. 99, 53–62.
Barker, J., Mitra, R., Griffiths, C., Dixit, V., Nickoloff, B., 1991. Keratinocytes as initiators of inflammation. Lancet 337, 211–214.
Baroli, B., Ennas, M.G., Loffredo, F., Isola, M., Pinna, R., Lopez-Quintela, M.A., 2007. Penetration of metallic nanoparticles in human full-thickness skin. J. Invest. Dermatol. 127, 1701–1712.
Belyakov, O.V., Mitchell, S.A., Parikh, D., Randers-Pehrson, G., Marino, S.A., Amundson, S.A., Geard, C.R., Brenner, D.J., 2005. Biological effects in unirradiated human tissue induced by radiation damage up to 1 mm away. Proc. Natl. Acad. Sci. 102 (40), 14203–14208.
Bettelli, E., Carrier, Y., Gao, W., Korn, T., Strom, T.B., Oukka, M., Weiner, H.L., Kuchroo, V.K., 2006. Reciprocal developmental pathways for the generation of pathogenic effector TH17 and regulatory T cells. Nature 441, 235–238.
Bing, R.J., 2001. Some aspects of biochemistry of myocardial infarction. Cell Mol. Life Sci. 58, 351–355.
Borm, P.J.A., 2002. Particle toxicity: from coal mining to nanotechnology. Inhal. Toxicol. 14, 311–324.
Boyle, W.J., Smeal, T., Defize, L.H., Angel, P., Woodgett, J.R., Karin, M., Hunter, T., 1991. Activation of protein kinase C decreases phosphorylation of c-Jun at sites that negatively regulate its DNA-binding activity. Cell 64 (3), 73–84.
Capusan, I., Mauksch, J., 1969. Skin disease of workers at a carbon-black-producing factory—with special reference to the 'carbon black' process. Berufs-Dermatosen 17 (28), 37.
Cavaleri, E.L., Rogan, E.G., 1992. The approach to understanding aromatic hydrocarbon carcinogensis. The central role of radical cations in metabolic activation. Pharmacol. Ther. 55, 183–199.

Cerruti, P.A., 1989. Response modification in carcinogenesis. Environ. Health Perspect. 81, 39–43.
Chabot-Fletcher, M., Breton, J., Lee, J., Young, P., Griswold, D., 1994. Interleukin-8 production is regulated by protein kinase C in human keratinocytes. J. Invest. Dermatol. 103, 509–515.
Chachami, G., Simos, G., Hatziefthimiou, A., Bonanou, S., Molyvdas, P.A., Paraskeva, E., 2004. Cobalt induces hypoxia-inducible factor-1alpha expression in airway smooth muscle cells by a reactive oxygen species-and PI3K-dependent mechanism. Am. J. Respir. Cell Mol. Biol. 31 (5), 544–551.
Chaudiere, J., Ferrari-Iliou, R., 1999. Intracellular antioxidants: from chemical to biochemical mechanisms. Food Chem. Toxicol. 37, 949–962.
Chiang, I.W., Brinson, B.E., Huang, A.Y., Willis, P.A., Bronikowski, M.J., Margrave, J.L., Smalley, R.E., Hauge, R.H., 2001. Purification and characterization of single-wall carbon nanotubes (SWNTs) obtained from the gas-phase decomposition of CO (HiPco Process). J. Phys. Chem. B 105 (35), 8297.
Chung, F., 2001. Anti-inflammatory cytokines in asthma and allergy: interleukin-10, interleukin-12, interferon-γ. Med. Inflamm. 10, 51–59.
Colburn, N.H., Former, B.F., Nelson, K.A., Yuspa, S.H., 1979. Tumour promoter induces anchorage independent irreversibility. Nature 281, 589–591.
Colburn, N.H., Lockyer, J., 1982. Phobol diester and epidermal growth factor receptors in 12-O-tetradecanoylphorbol-13-acetate-resistant and -sensitive mouse epidermal cells. Cancer Res. 42, 3093–3097.
Corsini, E., Galli, C., 1998. Cytokines and contact dermatitis. Toxicol Lett. 102–103, 277–282.
Curren, R.D., Mun, G.C., Gibson, D.P., Aardema, M.J., 2006. Development of a method for assessing micronucleus induction in a 3D human skin model (EpiDerm™). Mut. Res. 607, 192–204.
Dhar, A., Young, M.R., Colburn, N.H., 2002. The role of AP-1, NFkB, and ROS/NOS in skin carcinogenesis: the JB6 model is predictive. Mol. Cell Biochem. 234–235, 185–193.
Driscoll, K.E., Carter, J.M., Hassenbein, D.G., Howard, B., 1997. Cytokines and particle-induced inflammatory cell recruitment. Environ. Health Perspect. 105 (Suppl. 5), 1159–1164.
Eedy, D.J., 1996. Carbon-fibre-induced airborne irritant contact dermatitis. Contact Dermatitis 35, 362–363.
Eisen, M., Kaur, S., Rehema, A., Kullisaar, T., Vihalemm, T., Zilmer, K., Kaira, C., Zilmer, M., 2004. Allergic contact dermatitis is accompanied by severe abnormal changes in antioxidantivity of blood. Biomed. Pharmacother. 58, 260–263.
Enk, A.H., Saloga, J., Becker, D., Madzadeh, M., Knop, J., 1994. Induction of hapten-specific tolerance by interleukin 10 in vivo. J. Exp. Med. 179, 1397–1402.
Evelson, P., Ordonez, C.P., Llesuy, S., Boveris, A., 1997. Oxidative stress and in vivo chemiluminescence in mouse skin exposed to UVA radiation. J. Photochem. Photobiol. 38, 215–219.
Fraga, C.G., Oteiza, P.I., 2002. Iron toxicity and antioxidant nutrients. Toxicology 180, 23–32.
Fuchs, J., Huflejt, M., Rothfuss, L., Wilson, D., Caramo, G., Packer, L., 1989. Acute effects of near ultraviolet light on the cutaneous antioxidant defense system. Photochem. Photobiol. 50, 739–744.
Gorelik, O., Nikolaev, P., Arepalli, S., 2000. Purification procedures for single-walled carbon nanotubes. NASA Contractor Report, NASA, Hanover, MD (NASA/CR-2000-208926).
Grone, A., 2002. Keratinocytes and cytokines. Vet. Immunol. Immunopathol. 88, 1–12.
Haddad, J.J., Land, S.C., 2000. O_2-evoked regulation of HIF-1a and NFkB signaling and oxidative stress. Biochem. Biophys. Res. Commun. 323, 361–371.
Haddad, J.J., Olver, R.E., Land, S.C., 2000. Antioxidant/prooxidant equilibrium regulates HIF-1a and NFkB redox sensitivity. Evidence for inhibition by glutathione oxidation in alveolar epithelial cells. J. Biol. Chem. 275, 21130–21139.
Haddad, J.J., Harb, H.L., 2005. L-g-glutamyl-L-cysteinyl-glycine (glutathione; GSH) and GSH-related enzymes in the regulation of pro and anti-inflammatory cytokines: a signaling transcriptional scenario for redox(y) immunologic sensor(s)? Mol. Immunol. 42, 987–1014.
Halliwell, B., Cross, C.E., 1994. Oxygen-derived species: their relation to human disease and environmental stress. Environ. Health Perspect. 102, 5–12.
Honeywell-Nguyen, P.L., Gooris, G.S., Bouwstra, J.A., 2004. Quantitative assessment of the transport of elastic and rigid vesicle components and a model drug from these vesicle formations into human skin in vivo. J. Invest. Dermatol. 123, 902–910.
Jenkinson, H.A., 1997. Contact dermatitis in a chimney sweep. Contact Dermatitis 37, 35.
Kagan, V.E., Yalowich, J.C., Borisenko, G.G., Tyurina, Y.Y., Tyurin, V.A., Thampathy, P., Fabisiak, J.P., 1999. Mechanism-based chemopreventive strategies against etoposide-induced acute myeloid leukemia: free radical/antioxidant approach. Mol. Pharmacol. 56, 494–506.
Kasparov, A.A., Popova, T.B., Lebedeva, N.V., Gladkova, E.V., Gurvich, E.B., 1989. Evaluation of the carcinogenic hazard in the manufacture of graphite articles. Vopr. Onkol. 35, 445–450.
Kaur, S., Zilmer, M., Eisen, M., Rehema, A., Kullisaar, T., Vihalemm, T., Zilmer, K., 2004. Nickel sulphate and epoxy resin: differences in iron status and glutathione redox ration at the time of patch testing. Arch. Dermatol. Res. 295, 517–520.
Keane, R.W., Srinivasan, A., Foster, L.M., Testa, M.P., Ord, T., Nonner, D., Wang, H.G., Reed, J.C., Bredesen, D.E., Kayalar, C., 1997. Activation of CPP32 during apoptosis of neurons and astrocytes. J. Neurosci. Res. 48, 168–180.
Komarova, L.T., 1965. The effect of air contamination in the production of carbon black on the morbidity and health of the workers. Nauchn. Tr. Omsk. Med. Inst. 61, 115–121.
Lachapelle, J.M., 2002. Occupational airborne skin diseases. In: Kanerva, L., Elsner, P., Wahlberg, J.E., Maibach, H.I. (Eds.), Handbook of Occupational Dermatology. Springer-Verlag, Berlin, pp. 193–199.
Lademann, J., Weigmann, H.J., Rickmeyer, C., Barthelmes, H., Schaefer, H., Mueller, G., Sterry, W., 1999. Penetration of titanium dioxide microparticles in a sunscreen formulation into the horny layer and the follicular orifice. Skin Pharmacol. Appl. Skin Physiol. 12, 247–256.
Lansdown, A.B.G., 2001. Iron: a cosmetic constituent but an essential nutrient for healthy skin. Int. J. Cosm. Sci. 23, 129–137.
Lauer, A.C., Ramachadran, C., Lieb, L.M., Niemiec, S., Weiner, N.D., 1996. Targeted delivery to the pilosebaceous unit via liposomes. Adv. Drug Deliv. Rev. 18, 311–324.
Lepinski, J.A., Myers, J.C., 1995. Iron. In: Encylopedia of Chemical Technology, pp. 829–855.
Li, M.O., Flavell, R.A., 2008. Contextual regulation of inflammation: a duet by transforming growth factor-b and interleukin-10. Immunity 28, 468–476.
Lopez-Torres, M., Thiele, J.J., Shindo, Y., Han, D., Packer, L., 1998. Topical application of a-tocopherol modulates the antioxidant network and diminishes ultraviolet-induced oxidative damage in murine skin. Br. J. Invest. Dermatol. 138, 207–215.
Maritim, A.C., Sanders, R.A., Watkins III, J.B., 2003. Diabetes, oxidative stress and antioxidants: a review. J. Biochem. Mol. Toxicol. 17, 24–38.
Maynard, A.D., Baron, P.A., Foley, M., Shvedova, A.A., Kisin, E.R., Castranova, V., 2004. Exposure to carbon nanotube material: aerosol release during the handling of unrefined single walled carbon nanotube material. J. Toxicol. Environ. Health 67, 87–107.
McGeachy, M.J., Bak-Jensen, K.S., Chen, Y., Tato, C.M., Blumenschein, W., McClanahan, T., Cua, D.J., 2007. TGF-beta and IL-6 drive the production of IL-17 and IL-10 by T cells and restrain T(H)-17 cell-mediated pathology. Nat. Immunol. 8, 1390–1397.
McGeachy, M.J., Cua, D.J., 2008. Th17 differentiation: the long and winding road. Immunity 28, 445–453.
Meidan, V.M., Bonner, M.C., Michniak, B.B., 2005. Transfollicular drug delivery—is it a reality? Int. J. Pharm. 306, 1–14.
Meyer, M., Pahl, H.L., Bauerle, P.A., 1994. Regulation of the transcription factor NF-kB and AP-1 by redox changes. Chem.-Biol. Interact. 91, 91–100.
Monteiro-Riviere, N.A., Nemanich, R.J., Inman, A.O., Wang, Y.Y., Riviere, J.E., 2005. Multi-walled carbon nanotube interactions with human epidermal keratinocytes. Toxicol. Lett. 155 (3), 377–384.
Mossman, B.T., Churg, A., 1998. Mechanisms in the pathogenesis of asbestosis and silicosis. Am. J. Respir. Crit. Care Med. 157, 1666–1680.
Murray, A.R., Kisin, E.R., Kommineni, C., Vallyathan, V., Castranova, V., Shvedova, A.A., 2007. Pro/antioxidant status and AP-1 transcription factor in murine skin following topical exposure to cumene hydroperoxide. Carcinogenesis 28 (7), 1582–1588.
National Institute for Occupational Safety Health (NIOSH), 1978. Criteria for a Recommended Standard. Occupational Exposure to Carbon Black. U.S. Department of Health, Education, and Welfare, Rockville, MD, CDC, NIOSH.
Nickolof, B., 1991. The cytokine network in psoriasis. Arch. Dermatol. Res. 127, 871–884.
Nishi, J., Ogura, R., Sugiyama, M., Hidaka, T., Kohno, M., 1991. Involvement of active oxygen in lipid peroxide radical reaction of epidermal homogenate following ultraviolet light exposure. J. Invest. Dermatol. 97, 115–119.
Papavassiliou, A.G., Bohmann, K., Bohmann, D., 1992. Determining the effect of inducible protein phosphorylation on the DNA-binding activity of transcription factors. Anal. Biochem. 203 (2), 302–309.
Podda, M., Traber, M.G., Weber, C., Yan, L.J., Packer, L., 1998. UV-irradiation depletes antioxidants and cause damage in a model of human skin. Free Rad. Biol. Med. 24, 55–56.
Roco, M.C., Williams, S., Alivisatos, P., 2000. Nanotechnology research directions: IWGN workshop report. Kluwer, Dordrecht, the Netherlands.
Rockey, D.C., 2003. Vascular mediators in the injured liver. Hepatology 37, 4–12.
Rouse, J.G., Yang, J., Barron, A.R., Monteiro-Riviere, N.A., 2006. Fullerene-based amino acid nanoparticle interactions with human epidermal keratinocytes. Toxicol. In Vitro 20, 1313–1320.
Ryman-Rasmussen, J.P., Riviere, J.E., Monteiro-Riviere, N.A., 2006. Penetration of intact skin by quantum dots with diverse physicochemical properties. Toxicol. Sci. 91 (1), 159–165.
Schaefer, H., Watts, F., Brod, J., Illel, B., 1990. Follicular penetration. In: Scott, R.C., Guy, R.H., Hadgraft, J. (Eds.), Prediction of Percutaneous Penetration. Methods, Measurements, Modeling. IBC Technical Services, London, pp. 163–732.
Schins, R.P., Borm, P.J., 1999. Mechanisms and mediators in coal dust induced toxicity: a review. Ann. Occup. Hyg. 43, 7–33.
Schreck, R., Reiber, P., Baeuerle, P.A., 1991. Reactive oxygen intermediates as apparently widely used messengers in the activation of the NF-kappa-B transcription factor and HIV-1. EMBO J. 10 (8), 2247–2258.
Schreck, R., Baeuerle, P.A., 1991. A role for oxygen radicals as second messengers. Trends Cell Biol. 1 (2–3), 39–42.
Scott, C.D., Povitsky, A., Dateo, C., Gokcen, T., Willis, P.A., Smalley, R.E., 2003. Iron catalyst chemistry in modeling a high-pressure carbon monoxide nanotube reactor. J. Nanosci. Nanotechnol. 3, 63–73.
Shvedova, A.A., Kommineni, C., Jeffries, B.A., Castranova, V., Tyurina, Y.Y., Tyurin, V.A., Serbinova, E.A., Fabisiak, J.P., Kagan, V.E., 2000. Redox cycling of phenol induces oxidative stress in human epidermal keratinocytes. J. Invest. Dermatol. 114, 354–364.
Shvedova, A.A., Castranova, V., Kisin, E.R., Schwegler-Berry, D., Murray, A.R., Gandelsman, V.Z., Maynard, A., Baron, P., 2003. Exposure to carbon nanotube material:

assessment of nanotube cytotoxicity using human keratinocyte cells. J. Toxicol. Environ. Health A 66 (20), 1909–1926.
Sies, H., 1991. Oxidative stress: from basic research to clinical application. Am. J. Med. 91, 31S–38S.
Sinnott, S.B., Andrews, R., 2001. Carbon nanotubes: synthesis, properties, and applications. Crit. Rev. Solid State Mater. Sci. 26, 145–249.
Stumhofer, J.S., Silver, J.S., Laurence, A., Porrett, P.M., Harris, T.H., Turka, L.A., Ernst, M., Saris, C.J., O'Shea, J.J., Hunter, C.A., 2007. Interleukins 27 and 6 induce STAT3-mediated T cell production of interleukin 10. Nat. Immunol. 8, 1363–1371.
Subramoney, S., 1998. Novel nanocarbons—structure, properties, and potential applications. Adv. Mater. 10, 1157–1171.
Sugawara, T., Gallucci, R.M., Simeonova, P.P., Luster, M.I., 2001. Regulation and role of interleukin 6 in wounded human epithelial keratinocytes. Cytokine 15 (6), 328–336.
Tan, M.H., Commens, C.A., Burnett, L., Snitch, P.J., 1996. A pilot study on the percutaneous absorption of microfine titanium dioxide from sunscreens. Australas. J. Dermatol. 37 (4), 185–187.
Thiele, J.J., Traber, M.G., Tsang, K.G., Cross, C.E., Packer, L., 1997. In vivo exposure to ozone depletes vitamin C and E and induces lipid peroxidation in epidermal layers of murine skin. Free Rad. Biol. Med. 23, 385–391.
Thriene, B., Sobottka, A., Willer, H., Weidhase, J., 1996. Man-made mineral fibre boards in buildings—health risks caused by quality deficiencies. Toxicol. Lett. 88, 299–303.
Tinkle, S.S., Antonini, J.M., Rich, B.A., Roberts, J.R., Salmen, R., DePree, K., Adkins, E.J., 2003. Skin as a route of exposure and sensitization in chronic beryllium disease. Environ. Health Perspect. 111, 1202–1208.
Toledano, M.B., Leonard, W.J., 1991. Modulation of transcription factor NF-kappa B binding activity by oxidation–reduction in vitro. Proc. Natl. Acad. Sci. U.S.A. 88, 4328–4332.
Toll, R., Jacobi, U., Richter, H., Lademann, J., Schaefer, H., Blume-Peytavi, U., 2004. Penetration profile of microspheres in follicular targeting of terminal hair follicles. J. Invest. Dermatol. 123, 168–176.
Tyrrell, R.M., 1994. The molecular and cellular pathology of solar ultraviolet radiation. Mol. Aspects Med. 15, 1–77.
Van den Bergh, B.A., Bouwstra, J.A., Junginger, H.E., Wertz, P.W., 1999. Elasticity of vesicles affects hairless mouse skin structure and permeability. J. Control Release 62, 367–379.
Veldhoen, M., Hocking, R.J., Atkins, C.J., Locksley, R.M., Stockinger, B., 2006. TGFbeta in the context of an inflammatory cytokine milieu supports de novo differentiation of IL-17-producing T cells. Immunity 24, 179–189.
Vogt, A., Combadiere, B., Hadam, S., Stieler, K.M., Lademann, J., Schaefer, H., Autran, B., Sterry, W., Blume-Peytavi, U., 2006. 40 nm, but not 750 or 1,500 nm, nanoparticles enter epidermal CD1a+ cells after transcutaneous application on human skin. J. Invest. Dermatol. 126, 1316–1322.